FEMS **2025** EUROMAT

The effect of the replacement of La by Sr in $La_{1-x}Sr_xMnO_3$ perovskite on the catalytic oxidation of light hydrocarbons

C. Drosou[1], E. Nikolaraki[1], S. Fanourgiakis[1], C.K. Mytafides[1], V. Zaspalis[2,3], D.P. Gournis[1,4], I.V. Yentekakis[1, 4,*]

[1] *School of Chemical and Environmental Engineering, Technical University of Crete, 73100 Chania, Crete, Hellas*

[2] *Department of Chemical Engineering, Aristotle University of Thessaloniki, 54124 Thessaloniki, Hellas*

[3] *Chemical Process and Energy Resources Institute, Center for Research and Technology Hellas (CPERI/CERTH), 57001 Thermi, Thessaloniki, Hellas*

[4] *Institute of GeoEnergy /Foundation for Research and Technology-Hellas (IG/FORTH), 73100 Chania, Crete, Hellas*

* igentekakis@tuc.gr

INTRODUCTION

Perovskites, with general formula ABO_3, are highly promising materials in catalysis due to their excellent redox properties, high lattice oxygen ion mobility, and exceptional thermal stability. Their flexibility in replacing the A-site and/or B-site cations with other elements of the same or different valence (i.e., $A_{1-x}A'_xB_{1-x}B'_xO_{3\pm\delta}$) allows them to create oxygen defects (vacancies) and modify the valence state of the transition metals in the B-site. This, in turn, alters (a) the mobility of O_{2-} ions within the lattice and (b) their surface redox properties, thereby enhancing their catalytic performance.

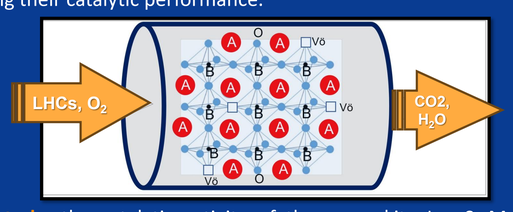

In the present study, the catalytic activity of the perovskite $La_{1-x}Sr_xMnO_3$ (LSxM), was comparatively examined for deep oxidation of light hydrocarbons, LHCs, namely CH_4, C_3H_8 and C_3H_6, under excess O_2 conditions. The effect of the gradual partial substitution of the A-site of $La_{1-x}A'_xMnO_3$ perovskite, (where A′ = Sr and x = 0, 0.3, 0.5, and 0.7) on the activity and stability of the materials in deep LHCs oxidation. Various characterization techniques such as BET, XRD, and H_2-TPR were employed to assess their physicochemical properties, correlating them with their catalytic activity. Additionally, different pre-treatment protocols were applied, including (a) pre-reduction, (b) pre-oxidation, and (c) oxidative aging at high temperatures.

EXPERIMENTAL

- LS_xM synthesis

- **Synthesis method**: Co-precipitation
- **Precursor compounds**: $La(NO_3)_3{\cdot}6H_2O$, $Sr(NO_3)_2$ & $Mn(NO_3)_2{\cdot}4H_2O$
- **Calcination temperature**: 1000 °C to obtain desired structure of perovskite
- $La_{1-x}Sr_xMnO_3$ (LSxM) where x= 0 – 70 (x represents % substitution of La by Sr) (**Table 1**)

- Catalyst Characterization Methods

- Structural and physicochemical characterization of LS_xM perovskites was conducted using BET, XRD and H_2-TPR techniques.

- Catalytic Activity & Stability Evaluation experiments

- A reactor unit with a tubular fixed-bed type reactor (quartz, ID = 3 mm)
- An analysis unit equipped with online gas chromatography (SHIMADZU GC-14B, a thermal conductivity detector)
- Three pre-treatment protocols for LSxM are as follows: (a) pre-oxidation at 400°C for 1 hour under 20% O_2/He flow, (b) pre-reduction at 600°C for 2 hours under 25% H_2/He flow, and (c) thermal oxidative "aging" at 750°C for 5 hours under 20% O_2/He flow.

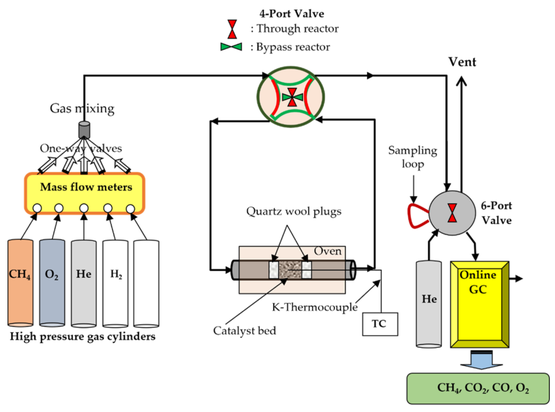

RESULTS & DISCUSSION

Table 1. A summary of LSxM chemical formulas, textural, morphological, and oxygen storage capacity characteristics.

	Chemical Formula	S_{BET} (m^2/g)	Pore diameter (nm)	OSC (μmol O_2 /g)
$LS_{00}M$	$LaMnO_3$	12.0	10.9	671
$LS_{30}M$	$La_{0.7}Sr_{0.3}MnO_3$	10.4	9.84	766
$LS_{50}M$	$La_{0.5}Sr_{0.5}MnO_3$	6.8	8.91	886
$LS_{70}M$	$La_{0.3}Sr_{0.7}MnO_3$	11.3	8.79	1219

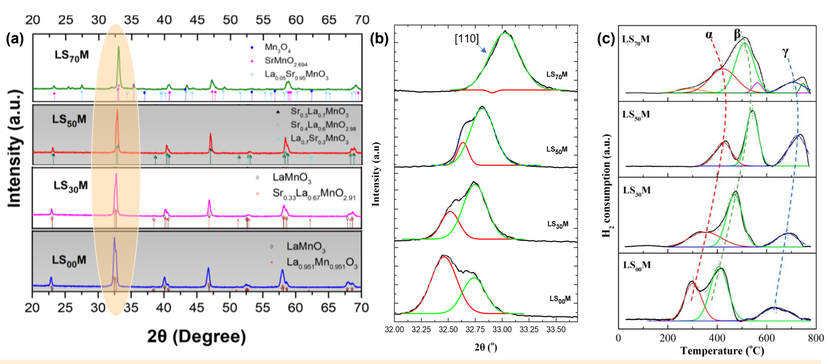

Fig. 1 (a) XRD patterns of LS_xM **(b)** magnification of XRD of LS_xM for 2θ=32-34° (where the main peak of the perovskite phase appears), **(c)** H_2-TPR profile of LS_xM perovskites (Peak **(α)** Oads, peak **(β)** reduction of Mn^{4+} to Mn^{3+}, peak **(γ)** → reduction of Mn^{3+} to Mn^{2+})

- CH_4 oxidation

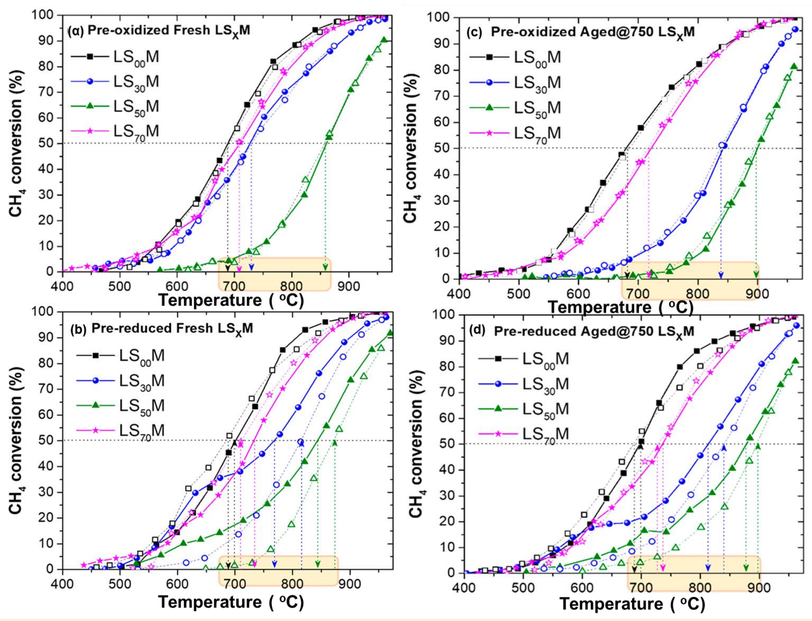

Fig. 2 Light-off/light-out behavior of pre-oxidized and pre-reduced (fresh (a, b) and aged at 750 °C (c, d) LS_xM catalysts, and their corresponding T_{50} values as a function of X. Feed conditions: 1.0% CH_4 + 5.0% O_2, He balance at 1 atm, WGHSV= 90,000 mL/g·h Solid symbols and lines show the heating path and open symbols, and the dashed lines show the cooling path of the cycle.

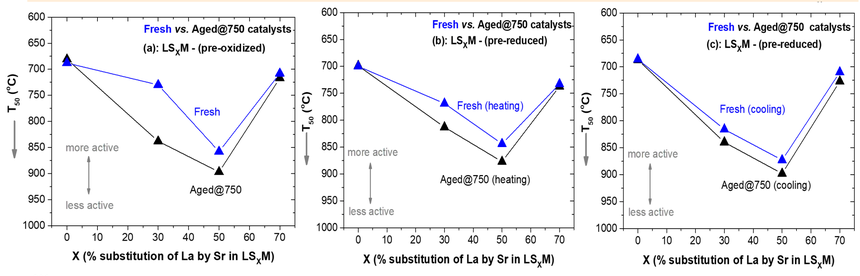

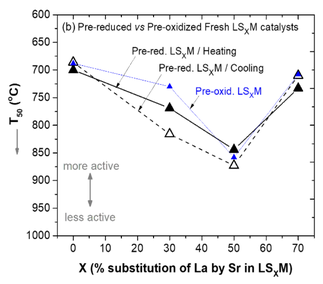

Fig. 3 Light-off/light-out behavior of pre-oxidized and pre-reduced (fresh (a, b) and aged at 750 °C (c, d) LS_xM catalysts, and their corresponding T_{50} values as a function of X. Feed conditions are shown, as in Fig. 2

- C_3H_6 oxidation

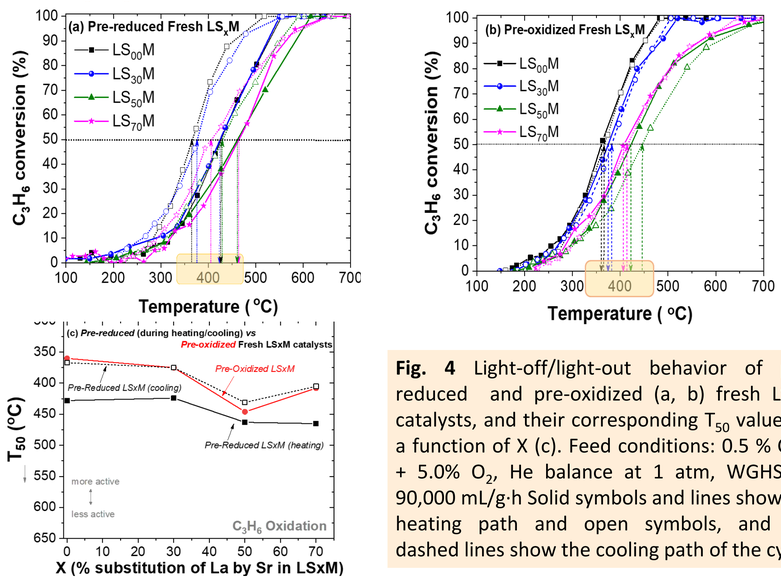

Fig. 4 Light-off/light-out behavior of pre-reduced and pre-oxidized (a, b) fresh LS_xM catalysts, and their corresponding T_{50} values as a function of X (c). Feed conditions: 0.5 % C_3H_6 + 5.0% O_2, He balance at 1 atm, WGHSV = 90,000 mL/g·h Solid symbols and lines show the heating path and open symbols, and the dashed lines show the cooling path of the cycle.

- C_3H_8 oxidation

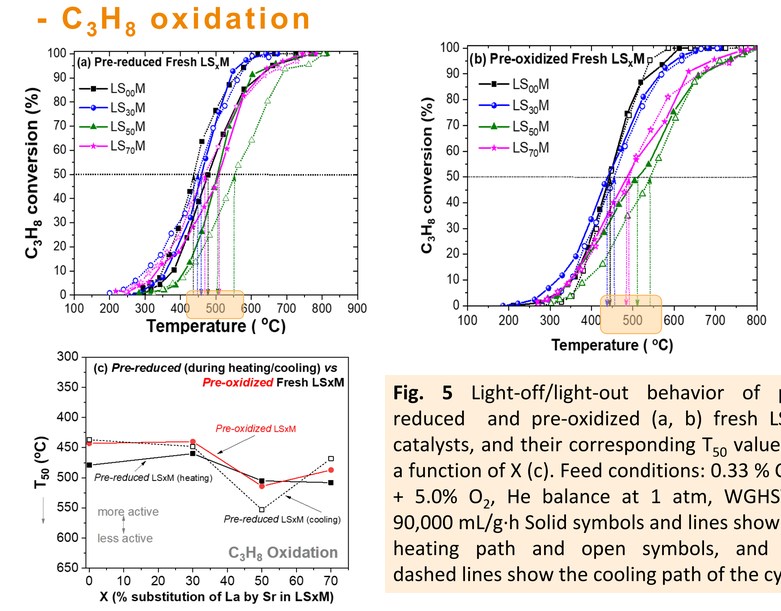

Fig. 5 Light-off/light-out behavior of pre-reduced and pre-oxidized (a, b) fresh LS_xM catalysts, and their corresponding T_{50} values as a function of X (c). Feed conditions: 0.33 % C_3H_8 + 5.0% O_2, He balance at 1 atm, WGHSV = 90,000 mL/g·h Solid symbols and lines show the heating path and open symbols, and the dashed lines show the cooling path of the cycle.

- Time-On-Stream (TOS) stability

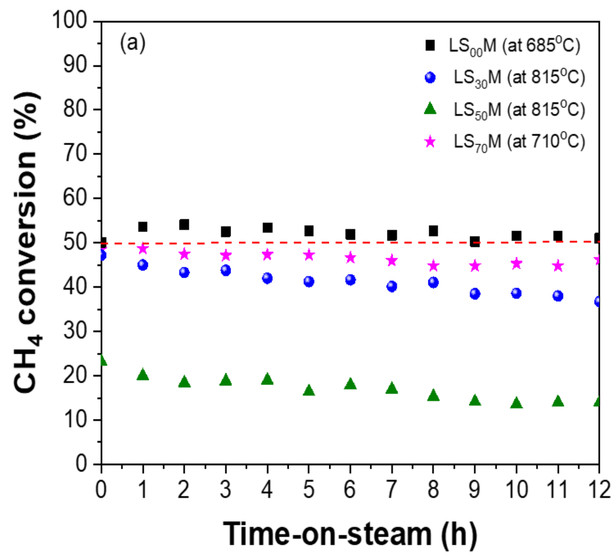

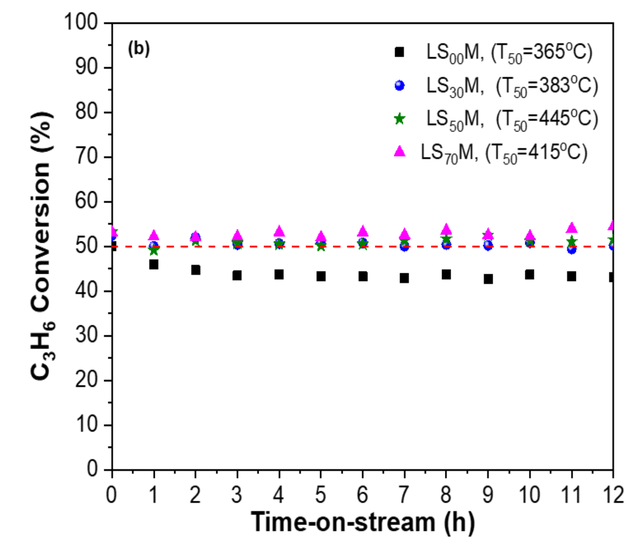

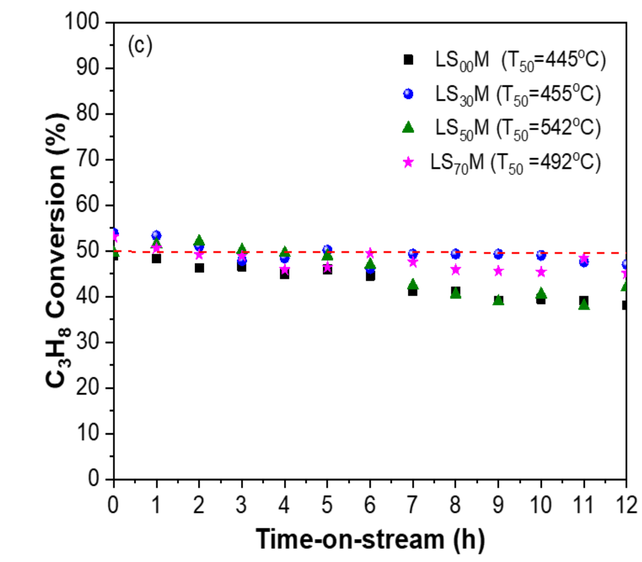

Fig. 6 Evaluation of the thermal stability of LS_xM catalysts at T_{50}, which is defined as the half-conversion temperature of CH_4 (a), C_3H_6 (b), and C_3H_8 (c). These experimental conditions correspond to Figures 2, 4, and 5.

CONCLUSIONS

- The degree of La substitution by strontium (Sr) consists the primary factor affecting the performance of LSxM catalysts .
- The catalytic performance of the materials followed an inverted volcano pattern based on the variable x, with the most efficient catalyst being for x=0 while the least efficient for x=0.5. This observation strongly **highlights the impact of x on the total surface area and the reducibility of the materials**.
- Complex **hysteresis phenomena** were recorded for the first time in the catalytic system during heating/cooling cycles, revealing new phenomena and findings that may be of interest to the catalysis under consideration.

REFERENCES

[1] He, C., Cheng, J., Zhang, X., […], Hao, Z. (2019). *Chem. Rev. 119, 4471-4568.*

[2] Drosou C., Nikolaraki E., Georgakopoulou T., […], Yentekakis I.V. (2023). *Nanomaterials 13, 2271* .

Acknowledgments

The research project is implemented in the framework of H.F.R.I call "Basic research Financing (Horizontal support of all Sciences)" under the National Recovery and Resilience Plan "Greece 2.0" funded by the European Union – NextGenerationEU. (H.F.R.I. Project Number: 16916)